

Quaternary Neptunium Compounds: Syntheses and Characterization of KCuNpS_3 , RbCuNpS_3 , CsCuNpS_3 , KAgNpS_3 , and CsAgNpS_3

Daniel M. Wells,[†] Geng Bang Jin,[†] S. Skanthakumar,[‡] Richard G. Haire,[§] L. Soderholm,[‡] and James A. Ibers^{*†}

[†]Department of Chemistry, Northwestern University, Evanston, Illinois 60208-3113, [‡]Chemical Science and Engineering Division, Argonne National Laboratory, Argonne, Illinois 60439, and [§]Chemical Sciences Division, Oak Ridge National Laboratory, Oak Ridge, Tennessee 37831

Received June 25, 2009

The five quaternary neptunium compounds KCuNpS_3 , RbCuNpS_3 , CsCuNpS_3 , KAgNpS_3 , and CsAgNpS_3 (AMNpS_3) have been synthesized by the reaction of Np, Cu or Ag, S, and K_2S or Rb_2S_3 or Cs_2S_3 at 793 K (Rb) or 873 K. These isostructural compounds crystallize as black rectangular plates in the KCuZrS_3 structure type in space group $Cmcm$ of the orthorhombic system. The structure comprises MS_4 ($M = \text{Cu}$ or Ag) tetrahedra and NpS_6 octahedra that edge share to form ${}_{\infty}^2[\text{MNpS}_3^-]$ layers. These layers are separated by the alkali-metal cations. The Np–S bond lengths vary from 2.681(2) to 2.754(1) Å. When compared to the corresponding isostructural Th and U compounds these bond distances obey the expected actinide contraction. As the structure contains no S–S bonds, formal oxidation states of $+1/+1/+4/-2$ may be assigned to A/M/Np/S, respectively. From these results a value of 2.57 for the bond-valence parameter r_0 for $\text{Np}^{4+}-\text{S}^{2-}$ has been derived and applied to the estimation of the formal oxidation states of Np in the binary Np_xS_y compounds whose structures are known.

Introduction

The solid-state chemistry of Np is thought to be intermediate between those of U and Pu, but the dearth of well-characterized examples of Np compounds remains an impediment to the full understanding of its chemistry. This is especially true for the non-oxide, non-neptunyl compounds where the stability of Np in multiple oxidation states is higher and such properties as superconductivity^{1,2} and non-Fermi liquid behavior^{3,4} have been observed. Np is produced both by the irradiation of U and as a byproduct in the production of important Pu isotopes. Understanding its chemistry is essential for efficient separations of spent nuclear fuel, addressing high-level radioactive waste, and production of special Pu isotopes.⁵ ${}^{237}\text{Np}$ has also been highlighted as a “burnable” isotope for future reactor fuels.⁵ In addition to

these aspects of Np chemistry, soft chalcogen-containing ligands have been used extensively in actinide organometallic and separations chemistry,⁶ and actinide chalcogenides have been investigated as potential fuels for future fast reactors.⁷ A fundamental understanding of Np chalcogenide solid-state chemistry is clearly relevant and is needed for these potential applications.

Even though many binary neptunium chalcogenides have been characterized by powder X-ray diffraction methods, only the cubic NpQ ($Q = \text{S}, \text{Se}, \text{or Te}$) compounds have been characterized by single-crystal X-ray diffraction methods.⁸ Most of the other known Np_xQ_y compounds resemble the corresponding U_xQ_y compounds and usually contain Np^{4+} , but some resemble the corresponding Ln_xQ_y compounds ($\text{Ln} = \text{rare-earth metal}$) and presumably contain Np^{3+} .⁹ Other than the Np_xQ_y compounds, NpTQ ($T = \text{O}, \text{As}, \text{or Sb}$; $Q = \text{S}, \text{Se}, \text{or Te}$),^{10–14} the superconducting Chevrel phase

*To whom correspondence should be addressed. E-mail: ibers@chem.northwestern.edu. Phone: +1 847 491 5449. Fax: +1 847 491 2976.

(1) Damien, D.; de Novion, C. H.; Gal, J. *Solid State Commun.* **1981**, *38*, 437–440.

(2) Aoki, D.; Haga, Y.; Matsuda, T. D.; Tateiwa, N.; Ikeda, S.; Homma, Y.; Sakai, H.; Shiokawa, Y.; Yamamoto, E.; Nakamura, A.; Settai, R.; Onuki, Y. *J. Phys. Soc. Jpn.* **2007**, *76*, 063701/1–063701/4.

(3) Stewart, G. R.; Kim, J. S.; Sykora, R. E.; Haire, R. G. *Physica B* **2006**, *378–380*, 40–43.

(4) Arko, A. J.; Joyce, J. J.; Havela, L. In *The Chemistry of the Actinide and Transactinide Elements*, 3rd ed.; Morss, L. R., Edelstein, N. M., Fuger, J., Eds.; Springer: Dordrecht, The Netherlands, 2006; Vol. 4, pp. 2307–2379.

(5) Yoshida, Z.; Johnson, S. G.; Kimura, T.; Krsul, J. R. In *The Chemistry of the Actinide and Transactinide Elements*, 3rd ed.; Morss, L. R., Edelstein, N. M., Fuger, J., Eds.; Springer: Dordrecht, The Netherlands, 2006; Vol. 2, pp. 699–812.

(6) Nash, K. L. *Solvent Extr. Ion Exch.* **1993**, *11*, 729–768.

(7) Allbutt, M.; Dell, R. M. *J. Nucl. Mater.* **1967**, *24*, 1–20.

(8) Wastin, F.; Spirlet, J. C.; Rebizant, J. *J. Alloys Compd.* **1995**, *219*, 232–237.

(9) Thévenin, T.; Pagès, M.; Wojakowski, A. *J. Less-Common Met.* **1982**, *84*, 133–137.

(10) Zachariasen, W. H. *Acta Crystallogr.* **1949**, *2*, 291–296.

(11) Charvillat, J. P.; Wojakowski, A.; Damien, D. *Proc. Int. Conf. Electron. Struct. Actinides*, 2nd **1976**, 469–473.

(12) Blaise, A.; Charvillat, J. P.; Salmon, P.; Wojakowski, A. *Proc. Int. Conf. Electron. Struct. Actinides*, 2nd **1976**, 475–481.

(13) Blaise, A.; Collard, J. M.; Fournier, J. M. *J. Phys., Lett.* **1984**, *45*, L-571–L-576.

(14) Wojakowski, A. *J. Less-Common Met.* **1985**, *107*, 155–158.

$\text{Np}_{1+x}\text{Mo}_6\text{Se}_8$,^{1,15} and the recently synthesized compound NpCuSe_2 ¹⁶ are known. The results of magnetic measurements suggest that the compounds NpTQ (T = As or Sb, Q = S, Se, or Te)^{11,13} and $\text{Np}_{1+x}\text{Mo}_6\text{Se}_8$ ^{1,15} contain Np^{3+} , but that the compounds NpOQ (Q = S and Se) contain Np^{4+} .^{17,18} On the basis of powder X-ray diffraction measurements the NpTQ compounds are isostructural to the corresponding U compounds, whereas the $\text{Np}_{1+x}\text{Mo}_6\text{Se}_8$ compound is isostructural to the corresponding Ln compounds. NpCuSe_2 is isostructural to known LnCuSe_2 compounds.¹⁶

The five quaternary compounds KCuNpS_3 , KAgNpS_3 , RbCuNpS_3 , CsCuNpS_3 , and CsAgNpS_3 presented here crystallize in the KCuZrS_3 structure type.¹⁹ This highly stable structure is unusual in its ability to accommodate both rare-earth and actinide elements in a wide variety of combinations of alkali- or alkaline-earth metals (A = K, Rb, Cs, Sr, or Ba) and mono- or divalent transition metals (M = Cu, Ag, Au, Mn, Co, Zn, Cd, Hg).^{20–30} For the actinides of formula AMAnQ_3 , the examples at this time are limited to combinations of A = K, Rb, Cs; M = Cu, Ag, Au; An = Th or U.^{31–36} Formal oxidation states here can be described as $\text{A}^{1+}\text{M}^{1+}\text{An}^{4+}(\text{S}^{2-})_3$. Thus, before this work no corresponding Np compounds were known and no Pu compounds are currently reported.

The bond-valence model, though empirical, has become popular throughout solid-state chemistry and material

science for its simplicity.³⁷ The method has found applications in crystallography, solid-state physics, mineralogy, and biology.³⁷ Extending this simplistic bonding model to actinide chemistry may help explain the stability of the many oxidation states found in the early actinides and expand our understanding of the localization or itineracy of the 5f electrons. The model has been extended to neptunyl, NpO_2^{n+} , compounds.^{38,39} Here we use the structural results on the title Np compounds to calculate the bond-valence parameter r_0 for $\text{Np}^{4+}-\text{S}^{2-}$ and then probe oxidation states in the known binary Np_xS_y compounds.

Experimental Section

General Syntheses. The following reagents were used as obtained from the manufacturer: K (Cerac, 98%), Rb (Strem, 99%), Cs (Aldrich, 99.5%), Cu (Aldrich, 99.5%), Ag (Aldrich, 99.99%), and S (Mallinckrodt, 99.6%). Brittle ²³⁷Np chunks (ORNL, 99.99%) were crushed and used as provided. The reactive fluxes⁴⁰ used in these syntheses, K_2S , Rb_2S_3 , and Cs_2S_3 , were prepared by stoichiometric reactions of the elements in liquid NH_3 .

Caution²³⁷Np is an α - and γ -emitting radioisotope and as such it is considered a health risk. Its use requires appropriate infrastructure and personnel trained in the handling of radioactive materials. To minimize the risk of reaction-vessel failures, all reaction vessels in this work consisted of primary and secondary containment. Primary containment was supplied by standard carbon-coated fused-silica ampules. Secondary containment comprised a combination of mechanical containment that consisted of stainless steel tubing with tongue and groove caps and chemical containment that was provided by a larger second fused-silica ampule. Further precautions were taken by heating all reactions in a computer-controlled high-temperature furnace equipped with both standard and runaway controllers. The furnace was located inside a negative-pressure hood.

Syntheses. KCuNpS_3 was prepared from a reaction mixture of 0.086 mmol Np, 0.086 mmol Cu, 0.043 mmol K_2S , and 0.258 mmol S. KAgNpS_3 was prepared from a reaction mixture of 0.084 mmol Np, 0.084 mmol Ag, 0.042 mmol K_2S , and 0.253 mmol S. RbCuNpS_3 was prepared from a reaction mixture of 0.0447 mmol Np, 0.253 mmol Cu, 0.294 mmol Rb_2S_3 , and 0.909 mmol S. CsCuNpS_3 was prepared from a reaction mixture of 0.084 mmol Np, 0.084 mmol Cu, 0.042 mmol Cs_2S_3 , and 0.126 mmol S. CsAgNpS_3 was prepared from a reaction mixture of 0.084 mmol Np, 0.042 mmol Ag, 0.101 mmol Cs_2S_3 , and 0.456 mmol S. For all the reactions the mixtures were loaded into carbon-coated fused-silica ampules in an Ar-filled drybox. These were evacuated to $\sim 10^{-4}$ Torr and flame-sealed. The reaction mixtures for KCuNpS_3 and KAgNpS_3 were heated to 873 K in 12 h, kept at 873 K for 144 h, cooled at ~ 3 K/h to 473 K, and finally cooled at 7.33 K/h to 298 K. The reaction mixture for RbCuNpS_3 was heated to 793 K in 20 h, kept at 793 K for 190 h, cooled to 423 at 1.95 K/h, and finally crash cooled to 298 K. The reaction mixtures for CsCuNpS_3 and CsAgNpS_3 were heated to 373 K in 4 h, kept at 373 K for 20 h, heated to 873 K in 6 h, kept at 873 K for 96 h, cooled at 4 K/h to 573 K, and finally crash cooled to 298 K. The reaction mixtures were removed from the inner ampules and placed under oil. All the AMNpS_3 compounds crystallized in approximately 10% yields as thin black rectangular plates. The crystals used in characterization were manually extracted from the product mixture. Owing to the

(15) de Novion, C. H.; Damien, D.; Hubert, H. *J. Solid State Chem.* **1981**, *39*, 360–367.

(16) Wells, D. M.; Skanthakumar, S.; Soderholm, L.; Ibers, J. A. *Acta Crystallogr., Sect. E: Struct. Rep. Online* **2009**, *65*, i14.

(17) Collard, J. M.; Blaise, A.; Bogé, M.; Bonnisseau, D.; Burlet, P.; Fournier, J. M.; Larroque, J.; Beauvy, M. *J. Less-Common Met.* **1986**, *121*, 313–318.

(18) Amoretti, G.; Blaise, A.; Bogé, M.; Bonnisseau, D.; Burlet, P.; Collard, J. M.; Fournier, J. M.; Quézel, S.; Rossat-Mignod, J.; Larroque, J. *J. Magn. Magn. Mater.* **1989**, *79*, 207–224.

(19) Mansuetto, M. F.; Keane, P. M.; Ibers, J. A. *J. Solid State Chem.* **1992**, *101*, 257–264.

(20) Wu, P.; Christuk, A. E.; Ibers, J. A. *J. Solid State Chem.* **1994**, *110*, 337–344.

(21) Huang, F. Q.; Choe, W.; Lee, S.; Chu, J. S. *Chem. Mater.* **1998**, *10*, 1320–1326.

(22) Yang, Y.; Ibers, J. A. *J. Solid State Chem.* **1999**, *147*, 366–371.

(23) Mitchell, K.; Haynes, C. L.; McFarland, A. D.; Van Duyne, R. P.; Ibers, J. A. *Inorg. Chem.* **2002**, *41*, 1199–1204.

(24) Mitchell, K.; Huang, F. Q.; McFarland, A. D.; Haynes, C. L.; Somers, R. C.; Van Duyne, R. P.; Ibers, J. A. *Inorg. Chem.* **2003**, *42*, 4109–4116.

(25) Mitchell, K.; Huang, F. Q.; Caspi, E. N.; McFarland, A. D.; Haynes, C. L.; Somers, R. C.; Jorgensen, J. D.; Van Duyne, R. P.; Ibers, J. A. *Inorg. Chem.* **2004**, *43*, 1082–1089.

(26) Yao, J.; Deng, B.; Sherry, L. J.; McFarland, A. D.; Ellis, D. E.; Van Duyne, R. P.; Ibers, J. A. *Inorg. Chem.* **2004**, *43*, 7735–7740.

(27) Strobel, S.; Schleid, T. *J. Alloys Compd.* **2006**, *418*, 80–85.

(28) Chan, G. H.; Sherry, L. J.; Van Duyne, R. P.; Ibers, J. A. *Z. Anorg. Allg. Chem.* **2007**, *633*, 1343–1348.

(29) Sikerina, N. V.; Andreev, O. V. *Russ. J. Inorg. Chem. (Transl. of Zh. Neorg. Khim.)* **2007**, *52*, 581–584.

(30) Chan, G. H.; Lee, C.; Dai, D.; Whangbo, M.-H.; Ibers, J. A. *Inorg. Chem.* **2008**, *47*, 1687–1692.

(31) Cody, J. A.; Ibers, J. A. *Inorg. Chem.* **1995**, *34*, 3165–3172.

(32) Sutorik, A. C.; Albritton-Thomas, J.; Hogan, T.; Kannewurf, C. R.; Kanatzidis, M. G. *Chem. Mater.* **1996**, *8*, 751–761.

(33) Huang, F. Q.; Mitchell, K.; Ibers, J. A. *Inorg. Chem.* **2001**, *40*, 5123–5126.

(34) Selby, H. D.; Chan, B. C.; Hess, R. F.; Abney, K. D.; Dorhout, P. K. *Inorg. Chem.* **2005**, *44*, 6463–6469.

(35) Yao, J.; Wells, D. M.; Chan, G. H.; Zeng, H.-Y.; Ellis, D. E.; Van Duyne, R. P.; Ibers, J. A. *Inorg. Chem.* **2008**, *47*, 6873–6879.

(36) Bugaris, D. E.; Ibers, J. A. *J. Solid State Chem.* **2009**, doi: 10.1016/j.jssc.2009.07.012.

(37) Brown, I. D. *The Chemical Bond in Inorganic Chemistry, The Bond Valence Model*; Oxford University Press: New York, 2002.

(38) Forbes, T. Z.; Wallace, C.; Burns, P. C. *Can. Mineral.* **2008**, *46*, 1623–1645.

(39) Albrecht-Schmitt, T. E.; Almond, P. M.; Sykora, R. E. *Inorg. Chem.* **2003**, *42*, 3788–3795.

(40) Sunshine, S. A.; Kang, D.; Ibers, J. A. *J. Am. Chem. Soc.* **1987**, *109*, 6202–6204.

Table 1. Crystal Data and Structure Refinements for KCuNpS₃, RbCuNpS₃, CsCuNpS₃, KAgNpS₃, and CsAgNpS₃^a

	KCuNpS ₃	RbCuNpS ₃	CsCuNpS ₃	KAgNpS ₃	CsAgNpS ₃
fw	435.82	482.19	529.63	480.15	573.96
<i>a</i> , Å	3.9616 (8)	3.9621 (2)	3.9644 (8)	4.058 (2)	4.0769 (4)
<i>b</i> , Å	13.862 (3)	14.3719 (9)	15.162 (3)	13.989 (6)	15.144 (2)
<i>c</i> , Å	10.234 (2)	10.2230 (6)	10.203 (2)	10.422 (4)	10.442 (1)
<i>V</i> , Å ³	562.0 (2)	582.13(6)	613.3 (2)	591.6 (4)	644.7 (1)
ρ _c , g/cm ³	5.151	5.502	5.736	5.391	5.914
μ, cm ⁻¹	238.6	306.3	270.4	223.9	254.6
absorption correction	face-indexed, SADABS	face-indexed, SADABS	face-indexed, SADABS	numerical, TWINABS	numerical, TWINABS
temperature, K	296 (2)	100 (2)	100 (2)	296 (2)	100 (2)
<i>R</i> (<i>F</i>) ^b	0.016	0.013	0.041	0.029	0.032
<i>R</i> _w (<i>F</i> _o ²) ^c	0.037	0.030	0.107	0.054	0.062

^a For all structures *Z* = 4, space group = *Cmcm*, λ = 0.71073 Å. ^b *R*(*F*) = $\sum ||F_o| - |F_c|| / \sum |F_o|$ for $F_o^2 > 2\sigma(F_o^2)$. ^c *R*_w(*F*_o²) = $\{\sum w(F_o^2 - F_c^2)^2 / \sum w(F_o^2)\}^{1/2}$ for all data. $w^{-1} = \sigma^2(F_o^2) + (qF_o^2)^2$ for $F_o^2 \geq 0$; $w^{-1} = \sigma^2(F_o^2)$ for $F_o^2 < 0$. *q* = 0.0228 for KCuNpS₃, 0.0141 for RbCuNpS₃, 0.0560 for CsCuNpS₃, 0.0229 for KAgNpS₃, and 0.0274 for CsAgNpS₃.

Table 2. Selected Interatomic Distances (Å) and Angles (deg) for KCuNpS₃, RbCuNpS₃, CsCuNpS₃, KAgNpS₃, and CsAgNpS₃

	KCuNpS ₃	RbCuNpS ₃	CsCuNpS ₃	KAgNpS ₃	CsAgNpS ₃
A–S1 × 2	3.182 (1)	3.2935 (8)	3.450 (5)	3.194 (2)	3.465 (2)
A–S2 × 4	3.3234 (9)	3.4128 (6)	3.545 (3)	3.401 (2)	3.538 (2)
A–S2 × 2	3.568 (1)	3.5988 (7)	3.661 (4)	3.524 (2)	3.699 (2)
M–S2 × 2	2.3169 (9)	2.3179 (7)	2.324 (4)	2.473 (2)	2.483 (2)
M–S1 × 2	2.3971 (9)	2.3943 (6)	2.397 (4)	2.547 (2)	2.544 (2)
Np–S1 × 2	2.7040 (6)	2.6915 (3)	2.681 (2)	2.754 (1)	2.7460 (9)
Np–S2 × 4	2.7051 (6)	2.7032 (4)	2.708 (3)	2.727 (1)	2.732 (1)
S2–M–S2	114.02 (5)	115.37 (4)	116.1 (2)	125.70 (8)	127.03 (9)
S2–M–S1	107.86 (2)	107.47 (1)	107.32 (7)	106.01 (3)	105.47 (3)
S1–M–S1	111.45 (6)	111.67 (4)	111.6 (2)	105.62 (9)	106.5 (1)
S1–Np–S2	89.57 (2)	89.55 (2)	89.8 (1)	85.96 (4)	86.17 (5)
S2–Np–S2	85.85(3)	85.75(2)	85.9(1)	83.85(6)	83.46(6)

difficulties of manipulating these samples no attempt was made to characterize the powders that remained.

Structure Determinations. Single-crystal X-ray diffraction data were collected with the use of graphite-monochromatized Mo Kα radiation (λ = 0.71073 Å) on a Bruker APEX II CCD diffractometer.⁴¹ The crystal-to-detector distance was 5.106 cm. The collection of the intensity data, cell refinement, and data reduction were carried out with the program APEX2.⁴¹ The crystals of both Ag compounds, KAgNpS₃ and CsAgNpS₃, were twinned; the multiple orientation matrices were determined with the use of the program CELLNOW,⁴² and the data were integrated in APEX2. For both, TWINABS⁴³ was used for separation of component reflections, numerical absorption correction, merging of data, and writing of the HKLF4 and HKLF5 format reflection files. Each structure was solved from the HKLF4 reflection file, and final least-squares refinement was completed with the use of the HKLF5 reflection file. For KCuNpS₃, RbCuNpS₃, and CsCuNpS₃ face-indexed absorption, incident beam, and decay corrections were completed with the use of the program SADABS.⁴⁴ All structures were solved with the direct-methods program SHELXS and refined with the least-squares program SHELXL.⁴⁵ Each final refinement included anisotropic displacement parameters. The program STRUCTURE TIDY⁴⁶ was then employed to standardize the atomic coordinates in each structure. Table 1 summarizes

crystal data and structure refinements and Table 2 presents selected metrical data. Additional information may be found in Supporting Information.

Bond Valence Sums. Bond valences, *V*_{*i*}, or estimated formal oxidation states,⁴⁷ were calculated from the formula $V_i = \sum_j \exp[(r_0 - r_{ij})/B]$, where the sum is over all *j* atoms in the first coordination sphere of atom *i*, with bond lengths *r*_{*ij*}. Here *r*₀ and *B* are bond-valence parameters. When standard parameters were available,^{37,48} the bond valences were calculated within the program PLATON;⁴⁹ for Np the program Bond Valence Calculator, Version 2.0⁵⁰ was used with *B* = 0.37, the standard *B* value for Th⁴⁺ and Uⁿ⁺. Given the distances determined for the present five AMNpS₃ compounds and a bond valence of +4 for Np, the above equation was solved for *r*₀ for each of those compounds, and the results were averaged to give *r*₀ = 2.57. A value of 2.57 also led to the minimum of $S = \sum (4 - V_i)^2$ over the range of *r*₀ values from 2.54 to 2.60, where the sum was over these five compounds.

Results

Syntheses. The compounds KCuNpS₃, KAgNpS₃, RbCuNpS₃, CsCuNpS₃, and CsAgNpS₃ have been synthesized in about 10% yields by the reactions of Np, Cu or Ag, S, and K₂S or Rb₂S₃ or Cs₂S₃ at 793 K (Rb) or 873 K.

Structures. The isostructural compounds KCuNpS₃, KAgNpS₃, RbCuNpS₃, CsCuNpS₃, and CsAgNpS₃

(41) Bruker. *APEX2 Version 2008.6-1 and SAINT Version 7.34a Data Collection and Processing Software*; Bruker Analytical X-Ray Instruments, Inc.: Madison, WI, 2006.

(42) Sheldrick, G. M. *CELLNOW*, 2008.

(43) Sheldrick, G. M. *TWINABS*, 2008.

(44) Bruker. *SMART Version 5.054 Data Collection and SAINT-Plus Version 6.45a Data Processing Software for the SMART System*; Bruker Analytical X-Ray Instruments, Inc., Madison, WI, 2003.

(45) Sheldrick, G. M. *Acta Crystallogr., Sect. A: Found. Crystallogr.* **2008**, *64*, 112–122.

(46) Gelato, L. M.; Parthé, E. *J. Appl. Crystallogr.* **1987**, *20*, 139–143.

(47) Brown, I. D.; Altermatt, D. *Acta Crystallogr., Sect. B: Struct. Sci.* **1985**, *41*, 244–247. The notation in that paper is used here.

(48) Brese, N. E.; O'Keeffe, M. *Acta Crystallogr., Sect. B: Struct. Sci.* **1991**, *47*, 192–197.

(49) Spek, A. L. *PLATON, A Multipurpose Crystallographic Tool*, 2008.

(50) Hormillosa, C.; Healy, S.; Stephen, T. *Bond Valence Calculator*, V2.0, 1993.

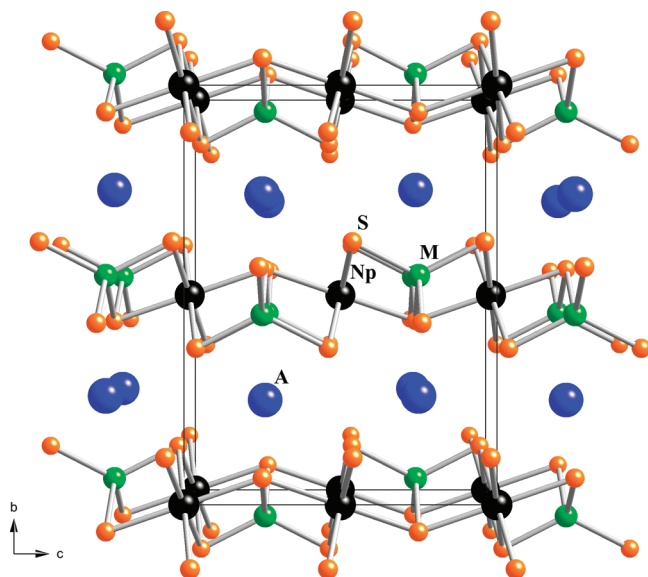


Figure 1. Structure of $AMNpS_3$ (A = alkali metal; M = coinage metal) viewed down $[100]$.

($AMNpS_3$) crystallize in the $KCuZrS_3$ structure type.¹⁹ The structure can be viewed as an alkali-metal intercalation or stuffed structure, previously described as the Cu(I) filled daughter of the $FeUS_3$, $AgTaS_3$, or Pd_3Te_2 structures.¹⁹ Another elegant *gedanken* experiment allows for a description of the structure as a daughter of the $ZrSe_3$ structure³⁴ that is also formed in binary Th, U, and Np chalcogenide phases.^{5,51} The structure comprises ${}_2^{\infty}[MNpS_3^-]$ layers alternating with alkali-metal cations stacked in the $[010]$ direction (Figure 1). The ${}_2^{\infty}[MNpS_3^-]$ layers are formed by alternating ribbons of NpS_6 octahedra and MS_4 tetrahedra. The NpS_6 octahedra edge share in the $[100]$ direction and corner share in the $[001]$ direction with other NpS_6 octahedra. The M atoms sit in tetrahedral holes, edge sharing with four Np octahedra in the (010) plane and corner sharing with two M tetrahedra in the $[100]$ direction. Each alkali metal is coordinated in a bicapped trigonal prismatic environment by eight S atoms. The shortest S–S interaction in the five compounds is 3.637(4) Å in $CsAgNpS_3$, much longer than a formal S–S single bond, for example, in US_3 (2.086(4) Å).⁵² As such, the formal oxidation states may be assigned for A/M/Np/S as +1/+1/+4/–2.

As in the isostructural U compounds, the structures display little variation within the ${}_2^{\infty}[MNpS_3^-]$ layers, only expanding in the (010) plane the necessary amount to accommodate the larger Ag^+ in place of Cu^+ . The c -axis expands by a much larger amount to accommodate the alkali-metal cations. In the Cu series, where three compounds have been synthesized, the c -axis scales linearly with the crystal radii of the cations.⁵³ Distances in the structures are normal, ranging from 2.3169(9) to 2.3971(9) Å for Cu–S, 2.473(2) to 2.547(2) Å for Ag–S,

Table 3. Oxidation States from Bond-Valence Analysis for Actinide Sulfide Compounds in the $KCuZrS_3$ Structure Type^a

compound	K, Rb, or Cs	Cu or Ag	Th, U, or Np
$KCuThS_3$	1.02	1.06	4.06
$KCuUS_3$	1.07	1.15	3.84
$KCuNpS_3$	1.10	1.16	4.17
$RbCuUS_3$	1.11	1.13	3.82
$RbCuNpS_3$	1.16	1.17	4.23
$CsCuUS_3$	1.28	1.12	3.82
$CsCuNpS_3$	1.37	1.15	4.24
$KAgNpS_3$	0.94	1.40	3.83
$RbAgUS_3$	0.99	1.37	3.49
$CsAgUS_3$	1.19	1.35	3.42
$CsAgNpS_3$	1.22	1.38	3.83

^a r_0 for $Np^{4+}-S^{2-}$ was taken as 2.57; standard values were used for $Th^{4+}-S^{2-}$ and $U^{4+}-S^{2-}$ (ref 48). Crystallographic data for the Th and U compounds were taken from ref 34 and ref 35, respectively.

3.182(1) to 3.568(1) Å for K–S, 3.2935(8) to 3.5988(7) Å for Rb–S, and 3.450(5) to 3.699(2) Å for Cs–S. These change very little from the isostructural U compounds where Cu–S bonds range from 2.321(2) to 2.413(1) Å, Ag–S from 2.490(2) to 2.552(2) Å, K–S from 3.190(3) to 3.585(2) Å, Rb–S from 3.310(2) to 3.626(2) Å, and Cs–S from 3.471(2) to 3.706(2) Å.³⁵ The most significant change in the structure occurs in the distortion of the M-tetrahedra upon substitution of Ag for Cu (Table 2).

Because this structure type is known for both rare-earth and actinide elements, it provides an excellent structure for the analysis through bond-distance comparisons of the preference of Np for trivalent or tetravalent oxidation states. The Np–S bonds in the present compounds range from 2.681(2) to 2.754(1) Å. In the series $KCuAnS_3$ the An–S bond distances decrease as one goes from Th, 2.7838(5) and 2.7872(2) Å,³⁴ to U, 2.7165(9) and 2.714(1) Å;³⁵ to Np, 2.7040(6) and 2.7051(6) Å. The trend fits well with the experimentally determined Wigner–Seitz radii for early actinides metals.⁵⁴ If Np were in formal oxidation state +3 in any of the present compounds then this trend would not apply and the Np–S bond lengths would approach those of the isostructural Nd compounds. In the Nd^{3+} compounds $BaNdCuS_3$ and $BaNdAgS_3$ the Nd–S bond distances are noticeably longer, ranging from 2.783(1) to 2.9011(9) Å.⁵⁵ The Np^{3+} –Se distance in $NpCuSe_2$ ¹⁶ differs from that in $NdCuSe_2$ ⁵⁶ by less than 0.021 Å. Clearly, the bond distances in the present compounds are consistent with Np being in the formal oxidation state +4, rather than +3. Of course, there is little ambiguity about the Ag oxidation state being +1 so the formula $AAgNpS_3$ requires Np^{4+} . On the other hand, it is conceivable that Cu could be in the +2 oxidation state in the present compounds. Not only is such a formulation inconsistent with the above comparisons but all known isostructural rare-earth/coinage metal compounds are formed with divalent alkaline-earth metal cations and not with monovalent alkali-metal cations.^{20–30}

Bond-Valence Analysis. Because the valence of Np in the present compounds can be assigned as +4, we have

(54) Wills, J. M.; Eriksson, O. *Los Alamos Sci.* **2000**, 26, 128–151.

(55) Bond distances were determined by fitting the structure to published lattice parameters from ref 20.

(56) Ijjaali, I.; Mitchell, K.; Ibers, J. A. *J. Solid State Chem.* **2004**, 177, 760–764.

(51) Grenthe, I.; Drozdynski, J.; Fujino, T.; Buck, E. C.; Albrecht-Schmitt, T. E.; Wolf, S. F. In *The Chemistry of the Actinide and Transactinide Elements*, 3rd ed.; Morss, L. R., Edelstein, N. M., Fuger, J., Eds.; Springer: Dordrecht, 2006; Vol. 1, pp 253–698.

(52) Kwak, J.; Gray, D. L.; Yun, H.; Ibers, J. A. *Acta Crystallogr., Sect. E: Struct. Rep. Online* **2006**, 62, i86–i87.

(53) Shannon, R. D. *Acta Crystallogr., Sect. A: Cryst. Phys. Diffr. Theor. Gen. Crystallogr.* **1976**, 32, 751–767.

Table 4. Bond-Valence Sums for Np_xS_y Compounds

compound	coordination	crystallo- graphic site	assigned oxidation state	bond valence	reference
Np_2S_3	7	Np1	3	3.96	10,62
	7	Np2	3	3.71	
Np_3S_5	8	Np1	3	3.11	61,65
	7	Np2	4	4.57	
Np_2S_5	10	Np	4	3.56	63,64
NpS_3	8	Np	4	4.93	62,63

calculated an r_0 value for KCuNpS_3 , RbCuNpS_3 , CsCuNpS_3 , KAgNpS_3 , and CsAgNpS_3 , respectively, and find the values 2.555, 2.549, 2.549, 2.586, and 2.587. We take these values to average 2.57 for the $\text{Np}^{4+}-\text{S}^{2-}$ bond. A bond-valence analysis of these five compounds along with those of the isostructural Th and U compounds is given in Table 3. The analysis works reasonably well, especially for the Cu-containing compounds. The structures of eight new U/S compounds^{55,57–59} have been published since the standard r_0 value for $\text{U}^{4+}-\text{S}^{2-}$ was last updated.⁶⁰ It is possible that inclusion of the distances in these structures would improve the analysis of valence, particularly for Ag/U/S compounds.

Table 4 details the bond-valence analysis for the binary Np_xS_y compounds. Also listed in Table 4 are oxidation states assigned to these compounds, mainly from the unique ²³⁷Np Mössbauer isomer shifts for Np^{3+} versus Np^{4+} .^{61,62} Np_2S_5 is thought to contain Np^{4+} owing to the actinide contraction.^{63,64} The bond-valence analysis tells us very little about the formal oxidation states of Np in these compounds, especially without comparison to a Np^{3+} bond-valence sum. This is perhaps not surprising given the wide variation in Np–S bond lengths for these

(57) Gray, D. L.; Backus, L. A.; Krug von Nidda, H.-A.; Skanthakumar, S.; Loidl, A.; Soderholm, L.; Ibers, J. A. *Inorg. Chem.* **2007**, *46*, 6992–6996.

(58) Zeng, H.-Y.; Yao, J.; Ibers, J. A. *J. Solid State Chem.* **2008**, *181*, 552–555.

(59) Yao, J.; Ibers, J. A. *Z. Anorg. Allg. Chem.* **2008**, *634*, 1645–1647.

(60) Brown, I. D., private communication.

(61) Thévenin, T.; Jové, J.; Pagès, M.; Damien, D. *Solid State Commun.* **1981**, *40*, 1065–1066.

(62) Thévenin, T.; Jové, J.; Pagès, M. *Hyperfine Interact.* **1984**, *20*, 173–186.

(63) Marcon, J.-P. *C. R. Seances Acad. Sci., Ser. C* **1967**, *265*, 235–237.

(64) Marcon, J.-P. *Commis. Energ. At. [Fr], Rapp.* **1969**, *CEA-R-3919*, 1–99.

(65) Marcon, J.-P.; Pascard, R. *Rev. Int. Hautes Temp. Refract.* **1968**, *5*, 51–54.

binaries,^{10,63–65} engendered, in part, by the presence of S_2^{2-} groups in some of these compounds. Once again, the analysis of bond valence in Np/S compounds might well improve as more experimental data become available.

Concluding Remarks

The first examples of quaternary Np/S compounds, namely, the compounds KCuNpS_3 , RbCuNpS_3 , CsCuNpS_3 , KAgNpS_3 , and CsAgNpS_3 synthesized in this work, more than double the number of well-characterized non-oxide quaternary Np compounds. The results also enable the determination of a bond-valence parameter of 2.57 for the $\text{Np}^{4+}-\text{S}^{2-}$ bond. The application of this value to the bond-valence analysis of binary Np_xS_y compounds adds little to our understanding of the charge distribution in these compounds.

Our initial attempts to synthesize the analogous AMNpSe_3 compounds were unsuccessful. It may be that the higher oxidizing potential of S compared to Se is needed to oxidize Np to Np^{4+} in this structure. Whereas the known Ae/M/U/Q compounds (Ae = alkaline-earth metal, M = coinage metal) contain U^{4+} but do not crystallize in the KCuZrS_3 structure type,^{58,59} it may be possible to synthesize the isostructural AeMNpQ_3 compounds. These compounds would contain Np^{3+} . It may also be possible to synthesize isostructural AMNpQ_3 compounds, where M is a divalent transition metal. Such compounds, which would also contain Np^{3+} , are known for the rare-earth metals.^{23–26,28,30,66}

Acknowledgment. This research was supported at Northwestern University by the U.S. Department of Energy, Basic Energy Sciences Grant ER-15522 and at Argonne National Laboratory by the U.S. Department of Energy, OBES, Chemical Science and Engineering Division, under contract DEAC02-06CH11357. D.M.W. wishes to thank the MRSEC program of the National Science Foundation (DMR-0520513) for support.

Supporting Information Available: Crystallographic files in CIF format for KCuNpS_3 , KAgNpS_3 , RbCuNpS_3 , CsCuNpS_3 , and CsAgNpS_3 . This material is available free of charge via the Internet at <http://pubs.acs.org>.

(66) Liu, Y.; Chen, L.; Wu, L.-M.; Chan, G. H.; Van Duyne, R. P. *Inorg. Chem.* **2008**, *47*, 855–862.